ELSEVIER

Chemical Engineering Journal 85 (2002) 197–206

Chemical Engineering Journal

www.elsevier.com/locate/cej

Experimental analysis of a single vapor bubble condensing in subcooled liquid

H. Kalman [a,*], Y.H. Mori [b]

[a] *Department of Mechanical Engineering, Pearlstone Center for Aeronautical Studies, Ben-Gurion University of the Negev, P.O. Box 653, Beer-Sheva 84105, Israel*

[b] *Department of Mechanical Engineering, Faculty of Science and Technology, Keio University, 3-14-1 Hiyoshi, Kohoku-ku, Yokohama 223-8522, Japan*

Received 18 April 2000; received in revised form 14 February 2001; accepted 19 February 2001

Abstract

An experimental investigation of the dynamics of, and the heat transfer to, the vapor bubbles condensing in a miscible or an immiscible liquid is presented in this paper. Unpublished experiments of Freon-113, pentane and hexane bubbles condensing in water and Freon-113 bubbles condensing in subcooled Freon-113 are analyzed and compared to previously published experiments of pentane/water, isopentane/water and pentane/glycerol systems. The experimental results of both the mechanical and thermal behaviors are compared to existing models. Throughout the comparison, we examine the effect of the shape and rigidity of condensing bubbles as well as the effects of the contaminants and noncondensibles on the velocity of, and the heat transfer to, the bubbles. Empirical correlations for the drag coefficient and the Nusselt number for a wide range of experimental parameters are developed. These correlations are simple to use (especially in contrast to existing complicated models requiring numerical solutions) and agree well with the experimental results.

Keywords: Condensation; Bubbles; Drag coefficient; Heat transfer coefficient

1. Introduction

Vapor bubble condensation is an important physical phenomenon emerging in a liquid–vapor two-phase flow when the liquid temperature is below the saturation temperature of the vapor species. Bubble collapse during condensation in immiscible liquids can be controlled either by inertia or by heat-transfer mechanisms. At a high liquid subcooling, bubbles rapidly collapse, satisfying the Rayleigh solution for the collapse of a spherical cavity in an infinite liquid in which the process is controlled by inertia of the surrounding liquid [1]. On the other hand, if subcooling is relatively low, the bubble collapse period will be longer and the process will be controlled by the heat transfer at the interface.

The collapse process in a heat-transfer controlled regime is a very complex phenomenon, as demonstrated in the scheme of Fig. 1. The collapse rate is generally assumed to be controlled by the internal and external thermal resistances and the temperature driving force. However, it can be affected by many parameters, as shown in Fig. 1. Bubbles might be condensed in both miscible and immiscible liquids. In the latter case, the condensate that remains in the bubble can take several different shapes, which have, respectively, different effects on the internal thermal resistance (all thermal resistances within the bubble). In some cases, the surface of each bubble might be mobile that is affected by the bubble size and its rising velocity, as shown in Fig. 1. In such a case, surface mobility will reduce both internal and external thermal resistances directly (through the boundary layers) and will change the condensate shape that is also affecting the internal thermal resistance. At high injection frequencies, a bubble might enter into the wake of the previous one, thus changing both the flow and temperature external fields. Due to this complexity, many theoretical models have been developed which address a few phenomena in a narrow range of parameters while neglecting others. A thorough theoretical analysis that would take into account all the parameters and possibilities seems to be impossible at this stage.

The direct contact condensation and collapse rate of single bubbles and bubble swarms have been intensively studied, both theoretically and experimentally [2–13]. Published experiments for bubbles condensing in miscible and immiscible liquids are listed in Table 1. Higeta et al. [12,13] showed visually that three patterns of condensation can be observed in immiscible liquids: (i) a condensate remains in

* Corresponding author. Tel.: +972-7-647-7099; fax: +972-7-647-2813.
E-mail address: kalman@menix.bgu.ac.il (H. Kalman).

1385-8947/02/$ – see front matter
PII: S1385-8947(01)00150-4

Nomenclature

C_D	drag coefficient
CFF	condensation of Freon-113 vapor in Freon-113
CFW	condensation of Freon-113 vapor in water
CHW	condensation of *n*-hexane vapor in water
C*i*PW	condensation of isopentane vapor in water
CMSO	condensation of methanol vapor in silicone oil
CPG	condensation of *n*-pentane vapor in glycerol
CPW	condensation of *n*-pentane vapor in water
CWSO	condensation of water vapor in silicone oil
D	volume-equivalent spherical diameter of bubble (m)
Eo	Eotvos number, $g\Delta\rho D^2/\sigma_L$
g	gravitational acceleration (m/s^2)
h	convective heat transfer coefficient based on ΔT defined by Eq. (20) or (21) (W/m^2 K)
h_{fg}	heat of vaporization (J/kg)
h^*	convective heat transfer coefficient based on ΔT defined by Eq. (19) (W/m^2 K)
H	defined in Eq. (13)
J	defined in Eq. (14)
k	thermal conductivity (W/m K)
m_v	mass of vapor (kg)
M	Morton number, $g\mu_L^4\Delta\rho/\rho_L^2\sigma_L^3$
Nu	Nusselt number, hD/k_L
Nu^*	Nusselt number, h^*D/k_L
Pe	Peclet number, UD/ν_L
Pr	Prandtl number, ν_L/α_L
R	radius of bubble ($=\frac{1}{2}D$) (m)
$\bar{R}$	normalized radius, R/R_0
$\bar{R}_f$	final normalized radius, R_f/R_0
R_0	initial radius (m)
R_{th_i}	internal thermal resistance that is the sum of all thermal resistances inside the bubble (K/W)
R_{th_o}	external thermal resistance that is the sum of all thermal resistances outside the bubble (K/W)
Re	Reynolds number, UD/ν_L
S	surface area (m^2)
t	time (s)
T	temperature (K)
ΔT	temperature driving force (K)
T_∞	temperature of continuous-phase liquid (K)
T_s	saturation temperature at vapor partial pressure (K)
T_s^*	saturation temperature at the system pressure (K)
U	rise velocity of bubble (m/s)
U_T	terminal velocity (m/s)

Greek symbols

α	thermal diffusivity (m^2/s)
μ	dynamic viscosity (Pa s)
μ_w	dynamic viscosity of water (Pa s)
ν	kinematic viscosity (m^2/s)
ρ	density (kg/m^3)
ρ_b	equivalent bubble density (kg/m^3)
σ_L	surface tension of continuous-phase liquid or effective surface tension working on the surface of two-phase bubble (N/m)

Subscripts

f	condensate or final state
L	continuous-phase liquid
v	vapor

each collapsing bubble, turning it into a stable two-phase bubble composed of a vapor core and a shell of the condensate; (ii) a large number of tiny particles of condensate form on the surface of each bubble and detach themselves from the bubble into the surrounding liquid; and (iii) a condensate grows in the form of several blunt drops at the rear part of the surface of each bubble. Mori [14] suggested which pattern of condensation actually emerges in a given immiscible

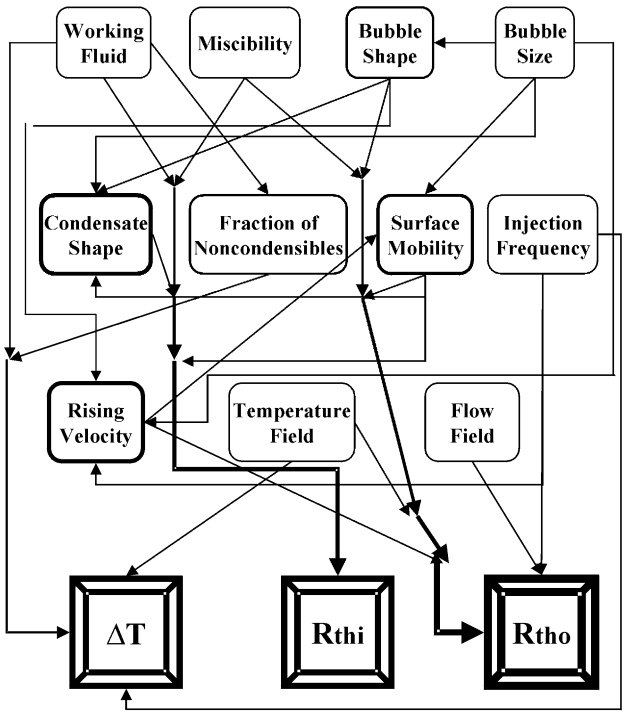

Fig. 1. Schematic presentation of the parameters affecting condensation. R_{th_i}: internal thermal resistance; R_{th_o}: external thermal resistance.

Table 1
Previously reported experiments of bubble condensation

Source	Dispersed phase	Continuous phase
Florschuetz and Chao [2]	Water Ethyl alcohol	Water Ethyl alcohol
Isenberg and Sideman [4]	Pentane Isopentane Pentane	Water Water Aqueous glycerol
Isenberg et al. [5]	Pentane Water	Pentane Water
Higeta et al. [12]	Pentane Water	Glycerol Silicone oil
Higeta et al. [13]	Methanol Water	Silicone oil Silicone oil + 1.82% ut. 1-decanol
Kalman et al. [9]	Pentane	Water
Lerner et al. [10]	Freon-113	Water
Kalman and Letan [11]	Freon-113	Freon-113
Chen and Mayinger [16]	Propanol Ethanol Water Freon-113	Propanol Ethanol Water Freon-113
Zeitoun et al. [18]	Water	Water

system is dependent on the spreading coefficient of the condensate on the bubble surface and, to a lesser extent, on the subcooling of the surrounding liquid. An extensive visualization study was conducted by Kalman et al. [9] and Lerner et al. [10], who showed that injected bubbles first accelerate and then decelerate. In the deceleration zone, the bubbles are enveloped by their own wakes. Based on this finding a theoretical "envelope model" was developed that agreed well with the experimental results.

Recently, Isikan [15] analyzed the collapse of spherical cap-shaped bubbles. Chen and Mayinger [16] used holographic interferometry and high-speed cinematograph to measure the heat transfer at the phase interface of a vapor bubble condensing in a subcooled liquid of the same substance. Wanchoo [17] developed an equation that predicts the Nusselt number and hence the collapse rate of large spherical bubbles condensing in immiscible liquids. Zeitoun et al. [18] developed interfacial transport models for subcooled steam–water bubbly flow in vertical conduits. Numerical solutions have been presented by Nigmatulin et al. [19] and Okhotsimskii [20].

The present paper deals with the dynamics of, and the heat transfer from, single vapor bubbles collapsing, under the control of the heat transfer, in a miscible or an immiscible liquid. The bubble collapse in an immiscible liquid is generally limited to the pattern in which each bubble turns into a stable two-phase bubble in which the condensate remains with a vapor phase yet to be condensed. Many experimental results from the literature as well as some new as-yet unpublished results of our own experiments are compiled from a comprehensive viewpoint, resulting in preparing new correlations for the bubble dynamics and the heat transfer. Those correlations seem to be a reasonable compromise between accuracy and ease of use for practical equipment design.

2. Experimental condensation rate and velocity

The new experiments were conducted using the apparatus described by Lerner et al. [10]. Although a theoretical model has been developed to predict the instantaneous bubble radius and velocity [9–11], polynomial curve fittings of experimental results are used in this paper for the sake of simplicity and in order to isolate the present analysis from any other effects and inaccuracies, which could have been imposed by the theoretical model. Consequently, the experimental measurements are described by fifth- and fourth-order polynomials for the instantaneous radius and height above the nozzle, respectively. These orders of the polynomial curves were selected to represent better the asymptotic behavior of the bubble radius toward the final radius and also to represent a slightly wavy change in the height with time. A typical example of such polynomial fittings to the experimental data is shown in Fig. 2. The instantaneous velocity of the bubble is calculated by differentiating the fourth-order polynomial correlation for the bubble location.

3. Bubble dynamics

The rise velocity of each bubble has been assumed by many researchers to be constant [2,4,7,15,18,21]. The assumption of constant velocity greatly contributes to simplifying their theoretical models of heat transfer controlled bubble collapse. Although the terminal velocity corresponding to the instantaneous radius of each bubble would inevitably change in the course of its collapse, the assumption of constant velocity may yield a reasonable approximation to the actual velocity history of the bubble in some circumstances. The actual velocity history in a given system should depend more or less on the bubble-feeding scheme employed there; this matter is briefly discussed below.

The bubble feeding schemes used in the previous studies may be classified into two. In one, each isolated bubble is first released into a mercury column maintained at a temperature slightly higher than the saturation temperature of the bubble-forming species, then breaks into an upper column of another lighter liquid which is subcooled below the saturation temperature (see, for example, Higeta et al. [12]). The initial velocity of the bubble in the upper column probably exceeds the terminal velocity for that bubble, resulting in its immediate deceleration together with the inception of condensation of the bubble-forming vapor over the bubble surface. In the other scheme, bubbles are directly injected at a low frequency into a subcooled liquid medium through

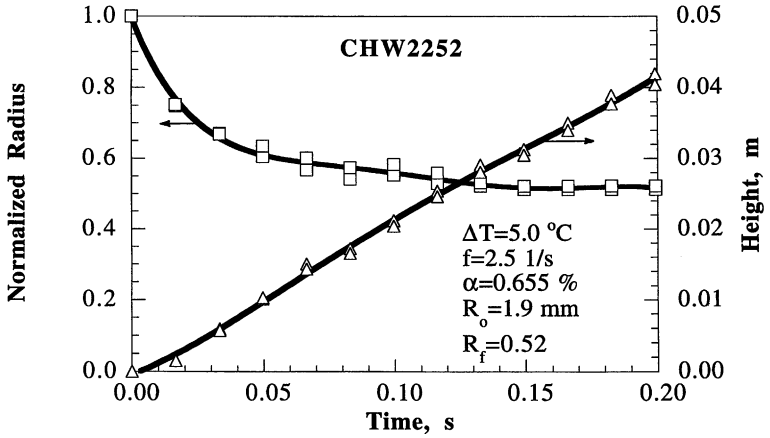

Fig. 2. Condensation rate and path of a representative bubble.

a nozzle submerged in it (see, for example, Kalman et al. [9]). In this case, each bubble starts to rise in the medium from rest or from a very low velocity generated in its growth/detachment process. Experiments showed that the condensing bubbles undergo an oscillatory shape deformation during the collapse process. The major shape deformation occurs at the initial stages of the collapse and is a result of the bubble detachment from the nozzle [22]. The bubble first accelerates, while collapsing at the same time, and then turns to a deceleration. The deceleration sometimes causes an envelopment of the bubble in its own wake [9].

The instantaneous force balance on a gravity-driven vapor–liquid bubble, taking into account buoyancy and drag forces, may be written as follows:

$$\frac{4}{3}\pi R^3\left(\rho_b+\frac{1}{2}\rho_L\right)\frac{dU}{dt} = \frac{4}{3}\pi R^3 g(\rho_L-\rho_b)-\pi R^2 C_D\frac{\rho_L U|U|}{2} \quad (1)$$

where R, U and ρ_b are the instantaneous radius, the velocity and the (total) density of the liquid–vapor bubble, respectively. C_D is the drug coefficient and ρ_L the density of the surrounding liquid. Eq. (1) includes the effect of the added mass due to the bubble motion. Eq. (1) was used first by Moalem-Maron et al. [23] and then adopted by Kalman et al. [9] and Lerner et al. [10]. Wanchoo [17] added an additional force due to the shrinkage of the bubble to the right-hand side of Eq. (1).

In order to calculate the rise velocity (whether it is assumed to be constant or time-dependent), the drag coefficient must be determined. Moalem-Maron et al. [23], followed by Lerner et al. [10], used

$$C_D=\frac{16}{Re}+\frac{6}{1+\sqrt{Re}}+0.4 \quad \text{for } 0<Re<2\times10^5 \quad (2)$$

for the drag coefficient. Wanchoo [17] used Haberman and Morton's finding for higher Reynolds numbers [24]

$$C_D=2.6 \quad \text{for } 10^3<Re<10^4 \quad (3)$$

and also from the correlation for lower ones due to Haas et al. [25]

$$C_D=\frac{14.9}{Re^{0.78}} \quad \text{for } 1<Re<10^3 \quad (4)$$

Higeta et al. [12] compared their experimental results obtained with pentane condensing in glycerol and water condensing in silicone oil to Stokes' and Oseen's theories for solid spheres:

$$C_D=\frac{24}{Re} \quad \text{for } Re<1 \quad (5)$$

$$C_D=\frac{24}{Re}\left(1+\frac{3Re}{16}\right) \quad \text{for } 0.3<Re<10 \quad (6)$$

They also compared their results to Hadamard and Rybczynski's theory and its extended version both for inviscid fluid spheres:

$$C_D=\frac{16}{Re} \quad \text{for } Re<1 \quad (7)$$

$$C_D=\frac{16}{Re}\left(1+\frac{Re}{8}\right) \quad \text{for } 1<Re<10 \quad (8)$$

Higeta et al. [12] found that concerning their rise motion, bubbles approximate inviscid fluid spheres at early stages of their collapse (or at relatively high Reynolds numbers), but act like rigid spheres at later stages of collapse (or at lower Reynolds numbers).

By assuming a quasi-steady-state condition the experimental drag coefficient can be derived from Eq. (1) to be

$$C_D=\frac{8}{3}\frac{Rg(\rho_L-\rho_b)}{\rho_L U^2} \quad (9)$$

where ρ_b is the bubble density and is defined as $\rho_b=\rho_v/\bar{R}^3$ for condensation in immiscible liquids and $\rho_b=\rho_v$ for condensation in miscible liquids. The instantaneous rise velocity of a bubble, U, is given by differentiating the polynomial curve-fitted to the data of instantaneous height of the bubble

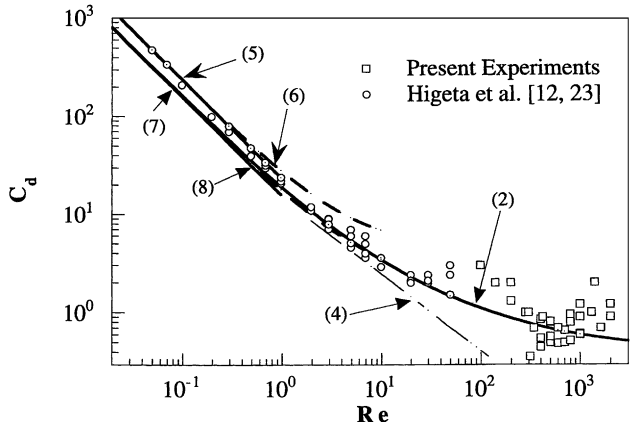

Fig. 3. Drag coefficient against Reynolds number: experimental results and theoretical lines.

in the test column (see Fig. 2). Substituting the $U(t)$ data thus prepared into Eq. (9) together with $R(t)$ data, we can evaluate C_D at discrete Re values in succession. Fig. 3 presents such experimental C_D values obtained by Higeta et al. [12] and Higeta [26] with pentane/glycerol system (CPG), water/silicone oil system (CWSO) and methanol/silicone oil system (CMSO), and those obtained in the present experiments with the following systems: Freon-113/water (CFW), pentane/water (CPW), hexane/water (CHW) and Freon-113/Freon-113 (CFF). Although the CWSO and CMSO systems do not give stable two-phase bubbles, the $C_D(Re)$ data for these systems are included in Fig. 3 because they follow the trend of $C_D(Re)$ of the other systems. Each data point in Fig. 3 represents the average of several neighboring $C_D(Re)$ data for some different runs deduced by the procedure described above. $C_D(Re)$ lines given by the above-listed correlations—Eqs. (2)–(8)—are also plotted in Fig. 3.

The correlation used by Moalem-Maron et al. [23] and Lerner et al. [10] (Eq. (2)) agrees reasonably well with the results of the experiments by Higeta et al. [12,23] as well as with some of the results from the present experiments. The latter experiments present higher drag coefficients both at the beginning of condensation process ($Re >$ 1000) and at the end of them ($Re <$ 200). This apparently irregular $C_D(Re)$ behavior exhibited by the collapse bubbles is not surprising, because even ordinary gas bubbles show such irregular behavior in the Re range between some 50 and 2000 [27] wherein their shape can significantly vary depending on Re (and also on other parameters such as Eo and M). Furthermore, the collapsing bubbles have some additional complexities which may affect their rise motions: first, each of them is strongly flattened right after its detachment from the nozzle, then falls to a shape oscillation, and second, the condensate accumulate at the rear of the bubble in later stages of its collapsing process undergoes a rocking motion, inevitably affecting its trajectory.

In their recent paper, Wanchoo et al. [28] showed $C_D(Re)$ data obtained with their experiments of vapor bubble collapse in immiscible liquids. To our surprise, their data falling in the range of $Re < 0.1$ indicate C_D values even lower than the corresponding values for inviscid fluid spheres, i.e. the values given by Eq. (7), thus strongly conflicting with the data of Higeta et al. [12]. Wanchoo et al. [28] insisted that such low C_D values are ascribable to the mobility of a condensate film and a strong circulation inside each two-phase bubble. However, we find no mechanistic reason to believe that the mobility of the condensate-film in the two-phase bubble exceeds that of the surface of a volume-equivalent inviscid fluid sphere, thereby causing a stronger internal circulation in the former than in the latter. At present, we have no reasonable explanation of the unusually low C_D values shown by Wanchoo et al. [28].

It is a general understanding that the drag coefficient C_D for bubbles rising in water medium is sensitive to the surface-active contaminants contained there, particularly in the regime of ellipsoidal bubble shape ($1 < D < 15$ mm); the $C_D(Re)$ curve for the bubbles can be either lower or higher than that for rigid spheres, depending on the degree of the contamination, as reviewed, for example, by Clift et al. [29]. For bubbles in the range $D > 1.3$ mm, Clift et al. [29] provided the following expression for U_T, the terminal velocity of bubbles, to represent its uppermost values available in highly purified systems

$$U_T = \left(\frac{2.14\sigma_L}{\rho_L D} + 0.505gD\right)^{1/2} \tag{10}$$

which is of the form suggested by Mendelson [30] based on an apparent similarity between the U_T versus D relation and the wave velocity versus wavelength relation, but includes empirically determined numerical factors. Although the validity of Eq. (10) has been confirmed only for air bubbles rising in purified water, we compare in Fig. 4 the U versus D data obtained in our experiments with $U_T(D)$ curves given by substituting into Eq. (10) the physical properties relevant

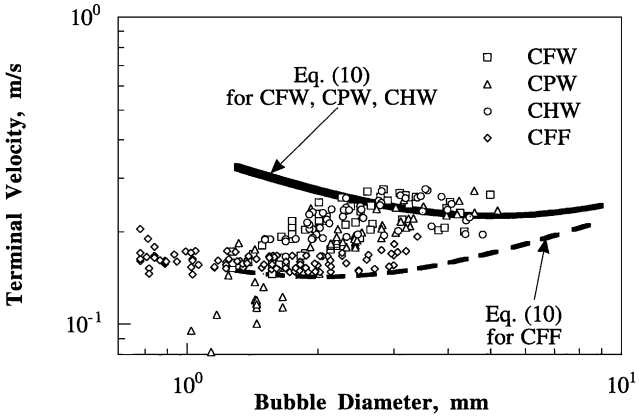

Fig. 4. Terminal velocity versus bubble diameter of the present experiments compared to Eq. (10).

to the CFF, CFW, CPW and CHW systems, respectively. In preparing the curves relevant to the CFW, CPW and CHW systems, we read σ_L as the sum of σ_f, the surface tension of the condensate, and σ_{Lf}, the water/condensate interfacial tension, assuming that a thin film of condensate covers a significant part of the surface of each two-phase bubble, thereby giving a duplex surface to the bubble. (The values of σ_f and σ_{Lf} at the saturation temperature under the atmospheric pressure were calculated from the correlations prepared by Watanabe and Okada [31] and Mori et al. [32], respectively.) The $U_T(D)$ curves of CFW, CPW and CHW systems are deviating from one another only slightly and hardly recognizable as separate curves. It is found that the experimental data for the CFF system are in reasonable agreement with (although slightly higher than) the relevant $U_T(D)$ curve given by Eq. (10). In contrast, the data for the CFW, CPW and CHW systems show D-dependencies, which are similar to each other, but considerably different from that indicated by Eq. (10). The U data for the three systems tend to fall below the relevant $U_T(D)$ curve with a decrease in D, i.e., with progress of collapse of the bubbles. One might assume the above tendency to be a feature of two-phase bubbles covered with liquid-condensate films. Our current opinion is, however, that the tendency is simply ascribable to the adsorption of surfactant contaminants on the water/condensate interface, i.e., the outer surface of each two-phase bubble; this is because σ_{Lf}, the inherent tension at the interface, is about three times as large as σ_f working on the surface of each vapor bubble in the CFF system, and hence once the surfactant adsorption sets in, the interface possibly induces a significant Marangoni force, thereby resisting (or reducing) its own tangential motion.

Grace et al. [33] recommended the following correlations for both bubbles and drops in contaminated systems in the range that $M < 10^{-3}$, $Eo < 40$ and $Re > 0.2$:

$$J = 0.94H^{0.757} \quad \text{for } 2 < H \leq 59.3 \tag{11}$$

$$J = 3.42H^{0.441} \quad \text{for } 59.3 < H \tag{12}$$

where

$$H = \frac{4}{3} Eo\, M^{-0.149} \left(\frac{\mu_L}{\mu_w}\right)^{-0.14} \tag{13}$$

$$J = Re\, M^{0.149} + 0.857 \tag{14}$$

and μ_w is a reference water viscosity to be taken as 0.9 mPa s. Since the bubble mechanics conditions of the present experiments are $M \cong 10^{-11}$, $0.2 < Eo < 10$ and $100 < Re < 2000$, an attempt has been made to replot the $U(D)$ data for the CFW, CPW and CHW systems in J–H coordinates for comparison with Eqs. (11) and (12). As shown in Fig. 5, the data are in a good agreement with Eqs. (11) and (12), again indicating a substantial effect of surfactant contaminants in the CFW, CPW and CHW systems employed in the experiments.

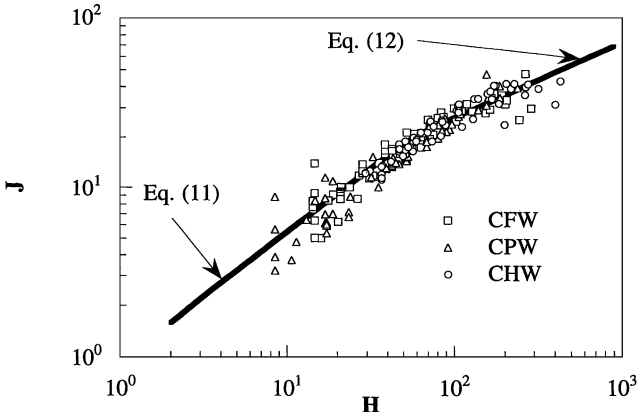

Fig. 5. Comparison between experimental J versus H and Eqs. (11) and (12).

The above examinations of formulating the rise motion of collapsing bubbles indicate a significant complexity of the mechanics of present concern, which is ascribable to the following facts:

1. the shape of bubbles is generally neither spherical nor invariable with time;
2. bubbles undergo unsteady shape oscillations, more or less depending on the dynamics of their injection into a liquid;
3. the liquid condensate accumulating in each bubble (in an immiscible system) may affect its rise motion more than would simply result from the increase in the effective bubble density, ρ_b, due to the condensate; and hence
4. both the mechanistic and the thermal situations inside and outside each bubble are highly time-dependent throughout the process of its collapse.

Therefore, it may be more practical to derive correlations for the drag coefficient exclusively based on relevant experimental results than referring to correlations mostly based on the observations of (noncollapsing) gas bubbles in motion. Following are the correlations we have prepared to conform to the collected $C_D(Re)$ data due to Higeta et al. [12,25] and to the present experiments:

$$C_D = \frac{24}{Re} + \frac{1}{5 + Re} + 1.5 \quad \text{for } 0.05 < Re < 100 \tag{15}$$

$$C_D = \frac{240}{Re} + 1.44 \times 10^{-5} Re^{1.5} \quad \text{for } 100 < Re < 2000 \tag{16}$$

As demonstrated in Fig. 6, the above correlations are in a reasonably good agreement with the experimental data. Eq. (16) presents a minimum of $C_D \approx 0.61$ at $Re \approx 658$, simulating an actual feature presumably due to competing effects of time-averaged bubble shape, shape oscillation, and surfactant contaminants accumulating at bubble surfaces. The Re and C_D values at the minimum point may be somewhat different from system to system, depending

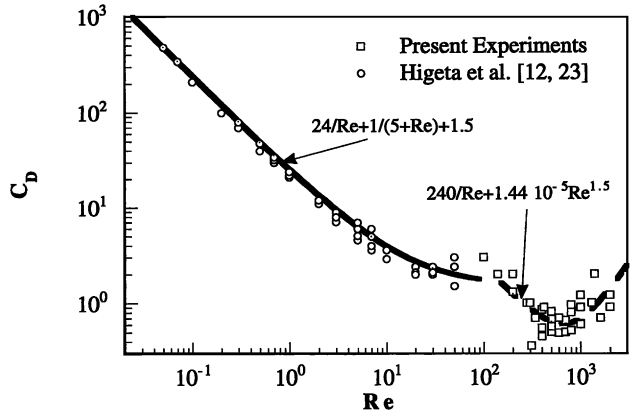

Fig. 6. Newly prepared empirical correlations for the drag coefficient, compared with experimental data.

on the chemical compound used as the continuous phase (particularly when water is used as the continuous phase). Clift et al. [29] showed that the deformation increases the drag coefficient of bubbles in contaminated water above the value of a rigid sphere if C_D and Re are based on the volume-equivalent diameter. Another explanation that relates to the collapsing-bubble deformation that increases rapidly when the Reynolds number is larger than the critical values, can be found in the work of Wanchoo et al. [28].

4. Heat transfer

Summarized in Fig. 7 are the experimental data of the instantaneous overall heat transfer coefficient related to the surface area of a sphere volume-equivalent to each two-phase bubble condensing in a miscible or an immiscible liquid. The heat transfer coefficient, h, is defined as follows by assuming a quasi-steady, convective heat release from each bubble caused by the instantaneous vapor condensation in it

$$hS\Delta T = -h_{fg}\frac{dm_v}{dt} \tag{17}$$

By inserting $m_v = \frac{4}{3}\pi R^3\rho_v$ and $S = 4\pi R^2$, Eq. (17) becomes

$$h = -\rho_v h_{fg}\frac{R_0}{\Delta T}\frac{d\bar{R}}{dt} \tag{18}$$

where the rate of collapse, $d\bar{R}/dt$, is derived from the polynomial fitted to the data for each collapse process (see Fig. 2). In this way, the heat transfer coefficient takes into account both internal and external thermal resistances. The temperature driving force can be defined in a number of ways. From an engineering point of view, the driving force is defined as the difference between the saturation temperature of the condensing species and the surrounding temperature, namely,

$$\Delta T = T_s^* - T_\infty \tag{19}$$

The content of noncondensibles in each bubble also affects the heat transfer coefficient. As the condensation progresses, the partial pressures of the noncondensibles increase and the partial pressure of the vapor decreases. Consequently, the saturation temperature also decreases. This is the reason why the condensation process ceases (i.e., the temperature driving force vanishes), still leaving a gaseous (gases plus vapor) phase integrated with a condensate phase. To take account of the effect of the noncondensibles, we define a modified temperature driving force as follows:

$$\Delta T = (T_s^* - T_\infty)\frac{\bar{R}^3 - \bar{R}_f^3}{\bar{R}^3 - (\rho_v/\rho_f)} \tag{20}$$

for condensation in immiscible liquids, and

$$\Delta T = (T_s^* - T_\infty)\frac{\bar{R}^3 - \bar{R}_f^3}{\bar{R}^3} \tag{21}$$

for condensation in miscible liquids, where $\bar{R}_f$ indicates the final normalized radius.

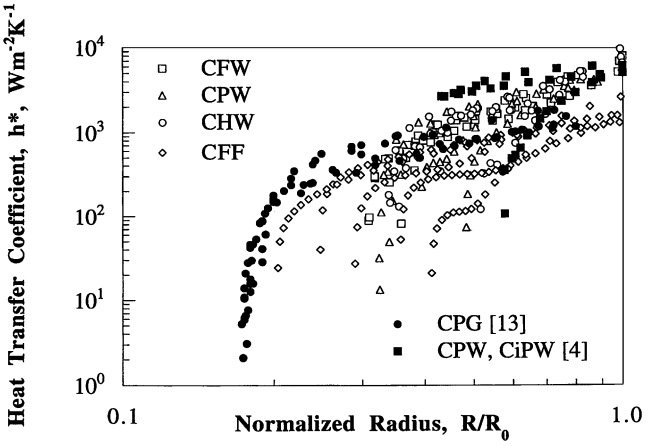

Fig. 7. Instantaneous convective heat transfer coefficient versus the normalized radius of bubbles.

Fig. 7 presents the experimental values of h^*, the heat transfer coefficient (disregarding the effect of noncondensibles) obtained by inserting Eq. (19) into Eq. (18). In the figure the present CFW, CPW, CHW and CFF experiments are compared to the previous experiments of Isenberg and Sideman [4] for pentane and isopentane bubbles condensing in water (CPW and C*i*PW, respectively) and the results of Higeta et al. [12] for pentane bubbles condensing in glycerol (CPG). The heat transfer coefficient for all the bubbles condensing in water start at nearly the same level and decreases sharply, without being scattered widely, toward the collapse termination. A moderate decrease in the heat transfer coefficient at early stages of collapse of each bubble is due to a combined effect of the increasing of the external thermal resistance (velocity decrease), the internal thermal resistance (condensate film thickening), and the partial pressures of

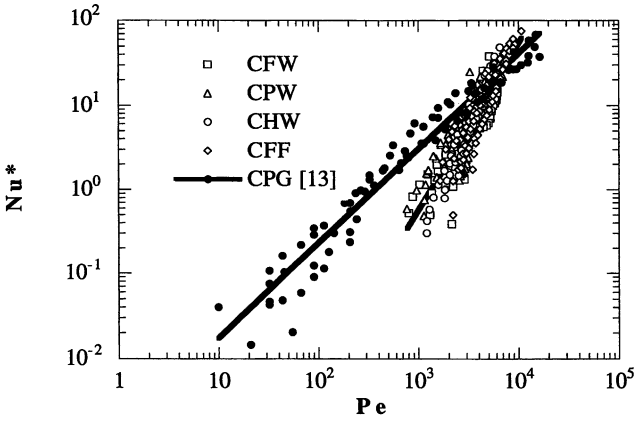

Fig. 8. Nusselt number (not rectified for eliminating the effect of the noncondensibles) versus Peclet number.

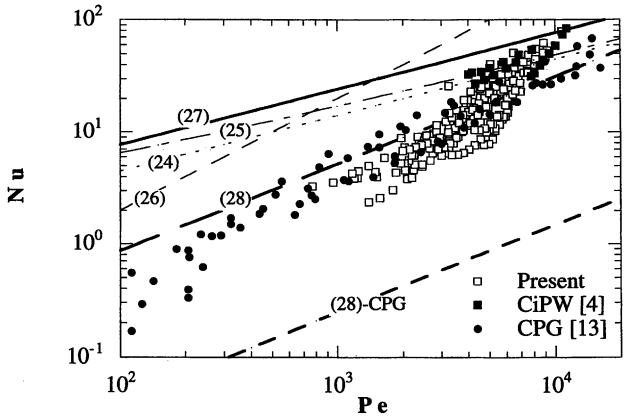

Fig. 9. Comparison between experimental data and previous correlations for Nusselt number.

noncondensibles. At final stages of collapse, a reduction of the temperature driving force controls the process. The data from the CFF experiments behave similarly to those for immiscible systems, although they start at a lower level due to the lower thermal conductivity of the surrounding liquid. The CPG experiments show a more moderate decrease in the heat transfer coefficient. It is also obvious from Fig. 7 that the CPG system used by Higeta et al. [12] was almost pure, containing little, if any, noncondensibles.

The experimental data shown above are replotted in Fig. 8 in a conventional, nondimensional form. Here, we note that the data for the CFF system overlap with those for the immiscible systems in which water is used as the continuous phase. This confirms the interpretation that the lower h^* values for the CFF system are mainly due to the lower thermal conductivity of the surrounding liquid, Freon-113. The decrease in Nu^* with a decreasing Pe is sharper in the present experiments than in the previous ones due to Higeta et al. [12], which is presumably ascribable to a difference in the amount of noncondensibles contained in the condensing fluids used. However, both experimental sets correlate reasonably with the power equation:

$$Nu^* = 1.31 \times 10^{-3}\, Pe^{0.95} \tag{22}$$

for the CPG data due to Higeta et al. [12] and

$$Nu^* = 6.88 \times 10^{-7}\, Pe^{1.97} \tag{23}$$

for the present results.

In order to eliminate the effect of the noncondensibles, we then employ Eq. (20) or (21), instead of Eq. (19), in evaluating the instantaneous temperature driving force, the heat transfer coefficient, h, and the Nusselt number, Nu. The data of the present experiments and those of previous ones for the C*i*PW [4] and for the CPG [12] systems are shown in Fig. 9. All of the data follow nearly the same Nu–Pe paths. The data in Fig. 9 are compared to the quasi-steady heat-transfer correlations some of which were used in bubble collapsing models reported previously. Those correlations are listed below.

Isenberg and Sideman [4] used

$$Nu = \frac{2}{\pi^{1/2}}(0.25\, Pr^{-1/3}\, Pe)^{1/2} \tag{24}$$

Clift et al. [29] suggested

$$Nu = 1 + \frac{0.752}{Pr^{0.139}}\left(1 + \frac{1}{Pe}\right) Pe^{0.472} \tag{25}$$

and Hori and Toda [34] defined their own correlation to be

$$Nu = 0.02\, Pe \tag{26}$$

Kalman et al. [9] and Lerner et al. [10] used, in their theoretical models, Lee and Barrow's correlations [35], which are

$$Nu = \frac{0.976}{Pr^{0.17}} Pe^{0.5} \tag{27}$$

for the front half of a rigid sphere, and

$$Nu = \frac{0.0447}{Pr^{0.45}} Pe^{0.78} \tag{28}$$

for the rear half. They also used the above correlations to calculate the external thermal resistance, which was to be added to an internal thermal resistance due to conduction through the condensate film.

Since most of the correlations depend also on Pr (aside from Pe), and the present experimental results cover the range of Pr from 3 to 7.5, the predictions by the above correlations were plotted for $Pr = 4$. Only Eq. (28) was plotted also for the CPG system, namely for $Pr = 3500$. It is seen that the predictions by Eqs. (24) and (25) are close to each other, and that they are in reasonable agreement with the experimental data at higher Peclet numbers. Eq. (26) gives Nu values about one order of magnitude higher than the data. Eqs. (27) and (28) are above and below, respectively, the experimental data at early stages of collapse, while both of them exceed the data at later stages. This fact supports the

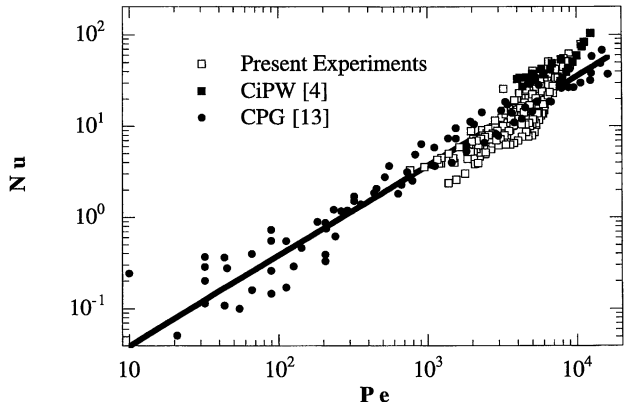

Fig. 10. Newly prepared empirical correlation for the Nusselt number compared with experimental data.

wake envelopment model of Kalman et al. [9] and Lerner et al. [10].

Although, many theoretical models describe the condensation process rather accurately, they all require a complicated analysis and numerical solutions. For engineering design procedures, we suggest the following correlation, since it represents reasonably, despite its highly simple form, all the data in a wide range of experimental parameters (see Fig. 10)

$$Nu = 0.0041\,Pe^{0.855} \tag{29}$$

This correlation is valid for condensation in both miscible and immiscible liquids for $0.05 < Re < 2000$ and $10 < Pe < 20{,}000$.

5. Conclusions

Experimental results, both existing and newly obtained, for bubbles condensing in miscible and immiscible liquids have been analyzed. Two empirical correlations for the drag coefficient were developed. The first correlation is applicable to $0.05 < Re < 100$ and the second to $100 < Re < 2000$. Taking account of the effect of noncondensibles on the temperature driving force, a single correlation for instantaneous heat transfer was developed which well agrees with the data from various systems and a wide range of experimental parameters. This simple correlation could be useful for engineering design purposes.

References

[1] L. Rayleigh, On the pressure development in a liquid during collapse of a spherical cavity, Phil. Mag. 34 (1917) 94–98.
[2] L.W. Florschuetz, B.T. Chao, On the mechanics of vapor bubble collapse, ASME J. Heat Transfer 87 (1965) 209–220.
[3] D.D. Wittke, B.T. Chao, Collapse of vapor bubbles with translatory motion, ASME J. Heat Transfer 89 (1967) 17–24.
[4] J. Isenberg, S. Sideman, Direct contact heat transfer with change of phase: bubble condensation in immiscible liquid, Int. J. Heat Mass Transfer 13 (1970) 997–1011.
[5] J. Isenberg, D. Moalem, S. Sideman, Direct contact heat transfer with change of phase: bubble collapse with translatory motion in single and two component systems, in: Proceedings of the Fourth International Heat Transfer Conference, Paris V, 1970.
[6] D. Moalem, S. Sideman, A. Orell, G. Hetsroni, Direct contact heat transfer with change of phase: condensation of bubble train, Int. J. Heat Mass Transfer 16 (1973) 2305–2319.
[7] H.R. Jacobs, H. Fannar, G.C. Beggs, Collapse of bubble of vapor in immiscible liquid, in: Proceedings of the Sixth International Heat Transfer Conference, Vol. 2, Hemisphere, Washington, DC, 1978, pp. 383–388.
[8] H.R. Jacobs, B.H. Major, The effect of noncondensible gases on bubble condensation in an immiscible liquid, ASME J. Heat Transfer 104 (1982) 487–492.
[9] H. Kalman, A. Ullmann, R. Letan, Dynamics of a condensing bubble in zones of time-dependent velocity, in: Proceedings of the Eighth International Heat Transfer Conference, Vol. 4, Hemisphere, Washington, DC, 1986, pp. 1925–1930.
[10] Y. Lerner, H. Kalman, R. Letan, Condensation of an accelerating–decelerating bubble: experimental and phenomenological analysis, ASME J. Heat Transfer 109 (1987) 509–517.
[11] H. Kalman, R. Letan, Condensation of a bubble in a miscible liquid: characteristics of the thermal resistance, in: Proceedings of the Ninth International Heat Transfer Conference, Vol. 3, Hemisphere, Washington, DC, 1990, pp. 3–8.
[12] K. Higeta, Y.H. Mori, K. Komotori, Condensation of a single vapor bubble rising in another immiscible liquid, AIChE Symp. Ser. 75 (189) (1979) 256–265.
[13] K. Higeta, Y.H. Mori, K. Komotori, A novel direct-contact condensation pattern of vapour bubbles in an immiscible liquid, Can. J. Chem. Eng. 61 (1983) 807–810.
[14] Y.H. Mori, Classification of configurations of two-phase vapor/liquid bubbles in an immiscible liquid in relation to direct-contact evaporation and condensation, Int. J. Multiphase Flow 11 (1985) 571–576.
[15] M.O. Isikan, Condensation of spherical-cap shaped bubbles, Int. J. Heat Mass Transfer 33 (1990) 1099–1103.
[16] Y.M. Chen, F. Mayinger, Measurement of heat transfer at the phase interface of condensing bubbles, Int. J. Multiphase Flow 18 (1992) 877–890.
[17] R.K. Wanchoo, Forced convection heat transfer around large two-phase bubbles condensing in an immiscible liquid, Heat Recovery Syst. CHP 13 (1993) 441–449.
[18] O. Zeitoun, M. Shoukri, V. Chatoorgoon, Interfacial heat transfer between steam bubbles and subcooled water in vertical upward flow, J. Heat Transfer 117 (1995) 402–407.
[19] R.I. Nigmatulin, N.S. Khabeev, F.B. Nagiev, Dynamics, heat and mass transfer of vapor–gas bubbles in a liquid, Int. J. Heat Mass Transfer 14 (1981) 1033–1044.
[20] A.D. Okhotsimskii, The thermal regime of vapor bubble collapse and different Jacob numbers, Int. J. Heat Mass Transfer 31 (1988) 1569–1575.
[21] S. Kamei, M. Hirata, Study on condensation of a single vapor bubble into subcooled water, Part 2—experimental analysis, Heat Transfer Jpn. Res. 19 (1990) 1–10.
[22] H. Kalman, A. Ullmann, Experimental analysis of bubble shape during condensation in miscible and immiscible liquids, J. Fluids Eng. 121 (1999) 496–502.
[23] D. Moalem-Maron, M. Sokolov, S. Sideman, A closed periodic condensation–evaporation cycle of an immiscible, gravity driven bubble, Int. J. Heat Mass Transfer 23 (1980) 1417–1424.
[24] W.L. Haberman, R.K. Morton, An experimental investigation of the drag and the shape of air bubbles rising in various liquids, David Taylor Model Basin Report No. 802, 1953.

[25] U. Haas, H. Schmidt-Traub, H. Brauer, Umströmung kugelförmiger blasen mit inner zirkulation, Chem. Ing. Tech. 44 (1972) 1060–1068.
[26] K. Higeta, Ph.D. Thesis, Keio University, Yokohama, 1982.
[27] T. Tadaki, S. Maeda, On the shape and velocity of single air bubbles rising in various liquids, Kagaku Kogaku 25 (1961) 254–264.
[28] R.K. Wanchoo, S.K. Sharma, G.K. Raina, Drag coefficient and velocity of rise of a single collapsing two-phase bubble, AIChE J. 43 (1997) 1955–1963.
[29] R. Clift, J.R. Grace, M.E. Weber, Bubbles, Drops and Particles, Academic Press, New York, 1978.
[30] H.D. Mendelson, The prediction of bubble terminal velocities from wave theory, AIChE J. 13 (1967) 250–253.
[31] K. Watanabe, M. Okada, Measurement of the surface tension of four halogenated hydrocarbons, CCl_3F, CCl_2F_2, $C_2Cl_3F_3$ and $C_2Cl_2F_4$, Int. J. Thermophys. 2 (1981) 163–176.
[32] Y.H. Mori, N. Tsui, M. Kiyomiya, Surface and interfacial tension and their combined properties in seven binary, immiscible liquid–liquid–vapor systems, J. Chem. Eng. Data 29 (1984) 407–412.
[33] J.R. Grace, T. Wairegi, T.H. Nguyen, Shape and velocities of single drops and bubbles moving freely through immiscible liquids, Trans. Inst. Chem. Engrs. 54 (1976) 167–173.
[34] Y. Hori, S. Toda, Condensation rate of vapour bubbles in subcooled flow in a vertical tube, in: Proceedings of the International Conference on Multiphase Flow'91, Tsukuba, Japan, 1991, pp. 161–164.
[35] K. Lee, H. Barrow, Transport process in flow around a sphere with particular reference to the transfer of mass, Int. J. Heat Mass Transfer 11 (1968) 1013–1026.